Microfabrics and textures of quartzites of the Indiavaí-Lucialva shear zone, SW Amazonian Craton: preliminary conclusions *Poster*

Harrizon Lima de Almeida[1] Amarildo Salina Ruiz[1] Axel Vollbrecht[2]

Introduction

The purpose of this contribution is to present preliminary results regarding the kinematics and deformation conditions of the Indiavaí-Lucialva Shear Zone, based on the analysis of the texture and microfabrics of related quartzites.

Geological setting

The Amazonian Craton consists of older Archean cores related to a larger accretionary event represented by the formation of several province belts (Teixeira et al. 1989; Tassinari et al. 2000). The tectonic evolution of the SW Amazonian Craton, in particular, has been attributed the formation of an accretionary complex, Proterozoic in age (Rodonia-San Ignacio Orogeny). Although that division was based on geochronologic data, lineaments have been proposed as structural limits between several terranes. Saes (1999) proposed that the Santa Helena and Jauru (Alto Jauru, Geraldes et al., 2001) terranes were separated by the Indiavai-Lucialva shear zone (ILSZ). The ILSZ constitutes an important mega structure which deformed units of the Jauru terrain and parts of the limit east of the Santa Helena terrain (Fig. 1). Based on field studies and Ar-Ar muscovite ages, Ruiz (2005) and Ruiz et al. (2005) have demonstrated that the ILSZ was formed during an extensional tectonic event, possibly associated with the rearrangement of collided blocks related to the Sunsás Orogeny (ca. 900 Ma).

[1] Dep. Geologia Geral, Universidade Federal de Mato Grosso-ICET/DGG [2] Geowissenschafliches Zentrum der Georg-August-Universität Göttingen (GZG)

The Indiavaí–Lucialva Shear Zone

The Indiavaí–Lucialva Shear Zone (ILSZ) strikes NW-SE over a distance of about 100 km separating magmatic rocks from a metavulcanic-metasedimentary sequence. In the studied area (Fig. 1) rocks which display a distinct mylonitic fabric frequently contain feldspar porphyroclasts and garnet. In addition, quartz-rich tectonites, former quartzites, developed along the ILSZ. The mylonitic foliation (s_{myl}) of these mylonitic quartizites, marked by aligned muscovite flakes and strongly flattened small quartz grains, is subparallel to the margins of the shear zone which strikes 315–330° and dips with angles between 60° and 70° to the east-northeast. Shear sense criteria are usually abundant mainly in gneisses which have retained evidence of mylonitization at mesoscale. Moreover, the rocks show a well-developed stretching lineation which is defined mainly by elongated grains of quartz and muscovite laths. The dip angles of this lineation typically vary between about 50° and 70°. The ILSZ clearly exhibits a normal fault kinematic, i.e. a top-to-the-NE movement, juxtaposing the Santa Helena Batholith against metavulcanic-metasedimentary sequences and orthogneisses of the basement.

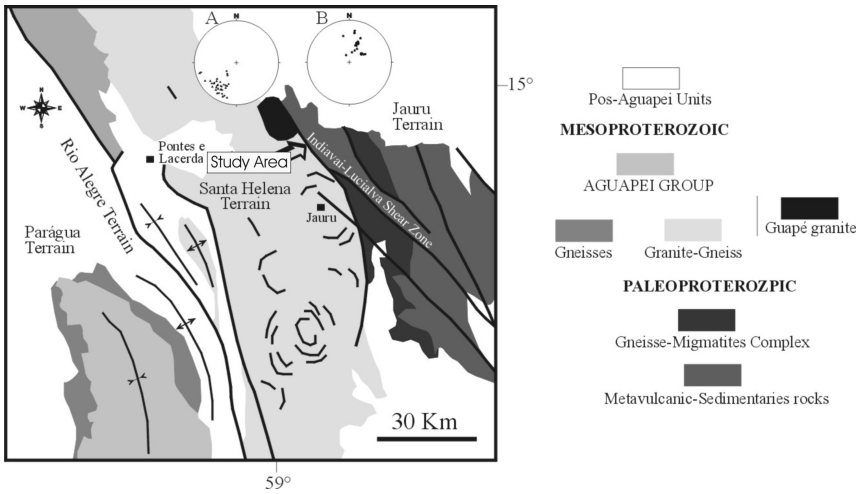

Figure 1: Geological sketch map of the SW Amazonian Craton. The stereoplots display the poles to the mylonitic foliation s_{myl} (A) and stretching lineation L (B), measured within the ILSZ; modified after Ruiz (2005).

Microfabrics

In all the analyzed quartzites, quartz forms polycrystalline aggregates consisting of inequigranular grains with very irregular interlobate grain boundaries. The average quartz grain size scatters between 0.3 and 1.4 mm (Fig. 2A). The occurrence of dissection microstructures (Urai et al. 1986) with the consequent formation of isolated 'island' grains, has also been observed in the several thin sections (Fig. 2A). Such microstructures are interpreted as resulting from fast migration of grain boundaries, correlated with the regime 3 microstructure of Hirth & Tullis (1992) which indicates high-temperature (HT) conditions during mylonitisation. In addition, other features pointing to grain boundary migration like dragging and pinning microstructures (Jessel, 1987) have been observed. Microstructures representing a subsequent intracrystalline deformation include deformation bands and irregular subgrains. Frequently, two sets of deformation bands are developed ('chessboard patterns'; Fig. 2B) indicating HT crystal plasticity (e.g., Kruhl, 1996). Muscovite occurs as solid inclusions in quartz or along the quartz grain boundaries. In the first case, muscovite consists of boudinaged single crystals elongated parallel to the mylonitic foliation (Fig. 2C). It also displays deformation (kink) bands, particulary within larger grains. Kinematic indicators, e.g. mica and tourmaline displaying distinct asymmetric fish-structures, point to a top-to-the-ENE (normal) sense of shear (Fig. 2D). Altogether, grain boundary migration has to be assumed here as the main mechanism of dynamic recrystallization.

Quartz textures

As a start, quartz *c*-axis textures (crystallographic-preferred orienta-

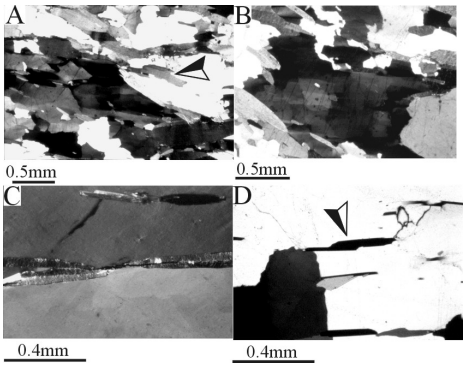

Figure 2: Deformation microstructures in mylonitic quartzite A. Quartz grains with irregular shape and lobate boundaries. The arrow points to an isolated 'island' grain. B. Two sets of deformation bands in quartz ('chessboard patterns'). C. Tourmaline (top) and muscovite grains (middle) showing boudinage. D. Tourmaline micro fish (arrow) documenting a top-to-the-east sense of shear when reoriented to the field.

tions) have been measured for three selected quartzite mylonite samples (Fig. 3). The quartz *c*-axis patterns are complex with a more or less pronounced asymmetry with respect to the reference directions (s_{myl} and L) indicating a predominance of non-coaxial deformation. The *c*-axis maxima close to s_{myl} suggest that prism slip in <a> or [c], which is generally attributed to HT deformation regimes (e.g. Mainprice et al. 1986), has significantly contributed to the texture development. Only sample C shows, in addition, a significant concentration of <c>-axes sub-normal to s_{myl} pointing to basal slip at lower temperatures. Intermediate positions of maxima are probably related to combined prism and basal slip in connection with complex deformation geometries (e.g. Garbutt & Teyssier, 1991). According to Stipp et al. (2002) complex pole figure of this

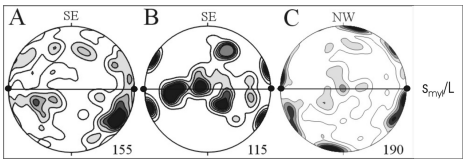

Figure 3: Quartz *c*-axis textures of three selected quartzite mylonites (A, B, C) from the ILSZ; horizontal line-trace of s_{myl}; dots — direction of L; trace of s_{myl} is oriented with respect to geographic directions; Schmidt net, lower hemisphere.

kind are typical for HT deformation of quartz polycrystals. As related to the field, the obliquity of the patterns indicates a top-to-the-NE sense of shear.

Conclusions

Based on both characteristic quartz microstructures and quartz *c*-axis textures the knowledge about the deformation conditions within the ILSZ could be improved. The microfabrics and intracrystalline structures of quartz indicate HT deformation with dominant grain boundary migration recrystallization and subsequent weak plastic deformation producing two sets of deformation bands in many grains. Deformation in a HT deformation regime is also confirmed by typical quartz *c*-axes textures which, in addition, reflect a strong component of non-coaxial strain.

Acknowledgements The research was supported by CNPQ Grant 350565/2004-0 and FAPEMAT Grant 3.2.2.33/02-2004.

References

Garbutt JM & Teyssier C (1991) Prism <c>-slip in quartzites of the Oakhurst Mylonite Belt, California. Journal Structural Geology 13: 657–666

Geraldes MC, Van Schmus W, Condie KC, Bell S, Teixeira W & Babinski M (2001) Proterozoic geologic evolution of the SW part of the Amazonian Craton in Mato Grosso state, Brazil. Precambrian Research 11: 91–128

Hirth G & Tullis J (1992) Dislocation creep regime in quartz aggregates. Journal Structural Geololy 2: 145–159.

Jessel MW (1987) Grain-boundary migration microstructure in a naturally deformed quartzite. Journal Structural Geology 9: 1007–1014

Kruhl JH (1996) Prism- and basal-plane parallel subgrain boundaries in quartz: a microstructural geothermobarometer. Journal Metamorphic Geolology 14: 581–589

Mainprice D, Bouchez JL, Blumenfeld P & Tubia JM (1986) Dominant c-slip in naturally deformed quartz: implications for dramatic plastic softening at high temperature. Geology 14: 819–822

Ruiz AS (2005) Evolução geológica do sudeste do Cráton Amazônico: região limítrofe Brasil-Bolívia. PHD Thesis. Unesp, Rio Claro, 250pp

Ruiz AS, Simões LSA, Almeida HL, Misson, AG & Manzano, JC (2005) Análise estrutural do batólito Santa Helena: implicações sobre a evolução tectônica do SW do Cráton Amazônico durante as orogenias San Ignácio-Rondoniano e Sunsás-Aguapeí. X Simpósio Nacional de Estudos Tectônicos. Curitiba, Brasil, 411–414

Saes G (1999) Evolução tectônica e paleogeográfica do aulacógeno Aguapeí (1.2–1.0 Ga) e dos terrenos do seu embasamento na porção sul do Cráton Amazônico. PHD Thesis. Usp, São Paulo, 135 pp

Stipp M, Stünitz H, Heilbronner R, Schmid S (2002) The eastern Tonale fault zone: a 'natural laboratory' for crystal plastic deformation of quartz over a temperature range from 250 to 700°C. Journal Structural Geology 24: 1861–1884

Tassinari CG, Bettencourt JS, Geraldes MC, Macambira MB & Lufon JM (2000) The Amazonian Craton. In: Cordani U, Milani EJ, Thomaz Filho A & Campos DA (ed) Tectonic Evolution of South América, I International Geological, Rio de Janeiro, Brazil, 41–95

Teixeira W, Tassinari CG, Cordani UG, Kawashita K (1989) A review of the geochronology of the Amazonian Craton: tectonic implications. Precambrian Research 42: 213–227

Urai JL, Means WS & Lister G (1986) Dynamic recrystallization of minerals. Geophysical Monographs 36: 161–199